Measurement of the spectrum of ultra-high energy cosmic rays by the Telescope Array surface array

A. Taketa*, M. Fukushima*, E. Kido*, K. Kasahara†, N. Sakurai*, H. Sagawa*, G. B. Thomson‡, B. T. Stokes‡, D. Ivanov‡ and S.Troitsky§ for the Telescope Array Collaboration

**Institute for Cosmic Ray Research, University of Tokyo, Kashiwa, Japan*
†*Waseda University, Okubo, Shinjuku-ku, Japan*
‡*Rutgers University, Piscataway, USA*
§*Institute for Nuclear Research of the Russian Academy of Sciences, Moscow, Russia*

***Abstract*. We present the energy spectrum of ultra-high energy cosmic rays based on the first year of data by the TA surface detector array.**

***Keywords*: Telescope Array, Surface Detector, EHECR spectrum**

I. Introduction

We built the Telescope Array (TA) experiment in Utah, USA, for the measurement of ultra-high energy cosmic rays. It is a direct extension of AGASA[1] and HiRes experiments[2], and both the surface detector (SD) array and the fluorescence detector (FD) are deployed in the same location to enable a simultaneous measurement. A cross calibration of the two measurement methods is possible using coincidence events. A full operation of TA began in March, 2008.

The array consists of 507 units of SD, each of which is composed of 2 layers of plastic scintillator with 1.2 cm thickness and 3 m^2 area. The SDs are deployed on a grid of 1.2 km spacing, and the whole array covers a ground area of approximately 700 km^2. Scintillation light is converted and guided to a PMT using a wave length shifting fiber and the PMT signal is digitized and recorded using a 12bit, 50 MHz FADC system. Waveforms of the top and the bottom scintillator is stored locally when both of them are hit with a pulse of more than $\sim$0.3 VEMs (Vertical Equivalent Muon). The rate of such coincidence is $\sim$700 Hz. The waveform of top-bottom coincidence event is integrated and histogrammed locally for the gain and linearity monitoring. Some of the stored waveforms are read out using the wireless communication when the shower event occurs. Such an event is triggered by the coincidence of 3 neighboring SDs, the energy deposition of which exceeds more than 3 VEMs.

II. Data Sample

We started a full operation of SD in March, 2008 as 3 independent branches of data acquisition (DAQ). They are integrated into a single array with branch crossing trigger and DAQ in November, 2008. In the present analysis, we use 14 months of SD data starting May 1st, 2008 until June 2009. The commissioning period until the end of April 2008 is discarded. The average duty cycle of DAQ in this period was 97% and the total exposure is approximately 1300 km^2 sr year, or 75% of the AGASA's exposure in 13 years.

For all the SDs, following checks are made using the monitor data, which is accumulated locally at the SD and transmitted every 10 minutes for the inspection.

1) Pedestal is stable with time and the distribution of the pedestal
2) The gain of SD is stable and in an appropriate range. The SD gain, described in the later section should be in between 6 and 54 ADC counts per MeV energy deposit. The average of all SDs is about 18 ADC counts per MeV.
3) Wireless LAN communication for the DAQ is stable: the packet loss rate should be smaller than 50% allowing 5 retries in the transmission.
4) The number of satellites seen by the GPS should be 3 or more than 3.
5) GPS time stamps of all the SDs are properly synchronized. The rate of desynchronization is however extremely low; less that once per day and per SD.
6) Deviation of the system clock frequency of each SD is to be within 5 counts (=100ns deviation). The measurement is made every 10 minutes. The average failure rate causing the rejection of 10 minutes DAQ period is $\sim 10^{-4}$ for one SD.
7) The buffering rate of SD waveform by the top and the bottom counter coincidence is between 500 and 1000 Hz, with its average being $\sim$700 Hz.

Only SDs which passed above checks and qualified normal are used for the subsequent analysis. The average of such 'good and normal' SDs is greater than 98% of the whole 507 SDs during the period of the analysis. The 'bad and discarded' SDs is not used for the event reconstruction, and its effect on the acceptance is taken into account in the air shower simulation.

An event sample is shown in Fig.1.

III. Calibration

Prior to the analysis, the calibration of the gain and the definition of usable FADC range is determined. The gain of the whole SD system is determined by the histogram

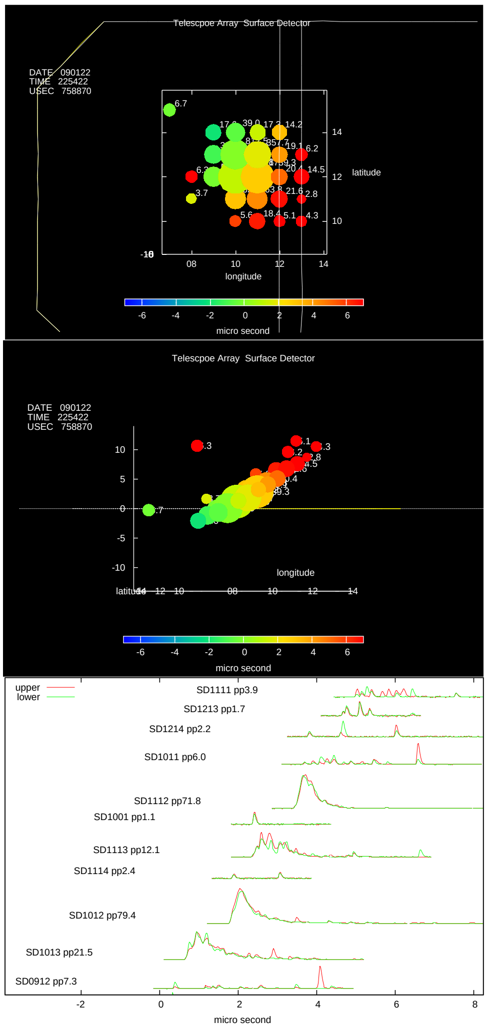

Fig. 1. An event sample acquired on 2009/01/22. The top figure is charge map, x-axis is longitude in detector id, y-axis is latitude in detector id, color bar represent triggered timing in micro second, diameter of each circle represent energy deposition. The middle figure is timing map, y-axis is triggered timing, x-axis is distance in detector id, color bar represent triggered timing in micro second, diameter of each circle represent energy deposition. The bottom figure is waveforms around shower core, solid line shows the top layer scintillator signal and dashed line shows the bottom layer's signal. The reason of less correlation of the top and the bottom layers (ex. SD1111 or SD0912) is caused by gamma ray and neutron.

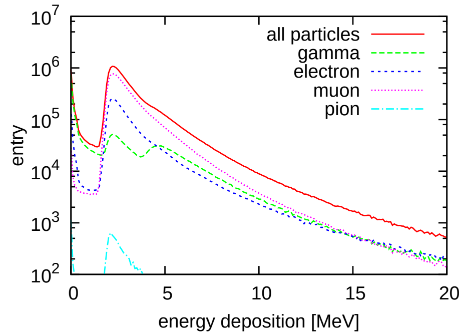

Fig. 2. Spectra of energy depositions by the simulation. solid-line : energy deposition spectrum by all particles, long-dashed-line : gamma rays, dashed-line : electrons, dotted-line : muons, chain-line : pions.

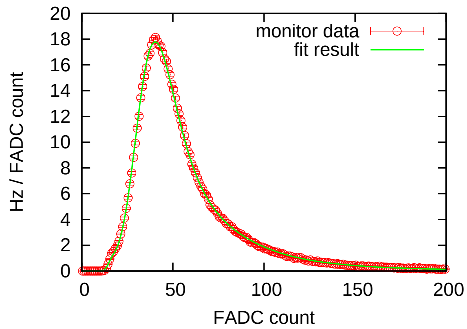

Fig. 3. Expected energy deposit by the simulation is shown by the solid line, and the measured spectrum is plotted by the open circle. The solid line is the result of fitting described in the text. The Detector gain of this counter was determined as 17.4 FADC counts per MeV energy deposit and the number of photo-electrons per MeV was estimated to be 20.4.

of the penetrating 'muon' accumulated locally at the SD. Pulse charges of ∼420k muons are histogrammed locally at the SD and sent out every 10 minutes for the recording. The counter gain G_M, which is the integrated FADC counts per unit energy deposit (MeV) in the scintillator, is determined from the monitor histogram as follows:

1) A distribution of particles on the ground is generated using COSMOS[3] MC and the energy spectrum of primary cosmic rays obtained by the extrapolation of the AMS spectrum[4]. Energy range of 3 GeV to 300 TeV, and the mass composition of proton, He and CNO are simulated.
2) An expected energy deposit (MeV) in the SD for such particle(s) is obtained using GEANT4 simulation[5]. The simulation demonstrated that most of the particles forming the peak of the histogram is muons (∼90%) and electrons (∼10%). See Fig.2.
3) The monitor histogram of the 'muon' (in FADC count) is fitted with the energy deposit histogram of GENAT4 (in MeV) with the G_M as the fit parameter. The energy deposit is smeared with SD impact point uniformity (7% fixed), single photo-electron resolution and the measured FADC noise. Also added (and fitted) are Poisson fluctuation of the number of photoelectrons. A typical result of the fitting is shown in Fig.3.

The results demonstrates that we are able to monitor and calibrate the SD gain at ∼1% level every 10 minutes for all the ∼1000 scintillators of TA.

The linear range of the SD was measured using a dual LED flashing system [6] before the deployment. The linear range by the LED is checked using the break point of the accumulated 'muon' histogram at the highest ADC counts region[6]. Both agree well. In the following data analysis, we discard any SD hit with a peak ADC count of more than 3000. This corresponds to a linear range in which the deviation from the linear response is within 7% for all the PMTs. This automatically takes care of the FADC overflow at 4095 counts.

For the event timing, we took a nominal GPS pps (pulse per second) timing prior to the event occurrence and a fractional time of one second is added using the DAQ 50 MHz system clock frequency measured within the second of event occurrence.

The absolute location and the altitude of each SD is measured by the GPS of each SD electronics operated in '3D fix mode' before the commissioning period. The accuracy is expected to be better than 0.3m in horizontal direction and less than 0.5m in altitude. After the commissioning period, the GPS is changed to 'position hold' mode and the accuracy of relative timing between far separated SDs in the field is expected to be within 20 ns[6]. In the present analysis, we use the array geometry database obtained by the above measurements. The timing of the SD waveform will be corrected for the altitude of each SD location for the data analysis.

IV. Data selection and Reconstruction

After the data quality cut and the calibration described above are applied, all the events are passed to the event selection and the shower reconstruction procedures.

1) Events with 4 or more effective SDs within a circle of 5 km diameter are selected. Here the effective SD means that it has at least one waveform (top or bottom) recorded within the linear range.
2) For each waveform, energy deposit within certain time window with respect to the signal timing (T10) is integrated. When two scintillators are available, we use an average of top and bottom counters. The 10% timing point T10, at which 10% of the total energy deposit is recorded, is calculated from the waveform. The timing of two counters are averaged as well.
3) We then fit the energy deposit and the T10 timing with a model function obtained from the MC simulation. Free parameters adjusted in the fitting are core locations (two parameters X and Y), arrival direction (two parameters, zenith and azimuthal angles of the shower axis) and the primary cosmic ray energy. The χ^2 cut is applied here.
4) We select events with the core location in the effective area of the array. Here, the edge of the effective area is defined as one 'layer' inside from the outermost SDs. For the analysis of energy spectrum, we plan to limit the zenith angle less than 45 degrees.

We used air shower model function produced by COSMOS MC in the above reconstruction procedure. The model function is composed of distribution of arrival timing $T(r, \phi, E, \theta)$ in the unit of nano second and its standard deviation $\Delta T(r, \phi, E, \theta)$, distribution of lateral energy deposit $Q(r, \phi, E, \theta)$ in the scintillator in the unit of MeV and its rms deviation $\Delta Q(r, \phi, E, \theta)$. Here, r, E, θ, ϕ are distance from the core location on the ground in the unit of m, the energy of the primary particle in the unit of eV and the zenith and the rotation angle measured from the projection of shower axis on the ground, respectively. Air showers are generated using a new hybrid method described in [7]. The energy deposition and its rms deviation at each SD are obtained using the GEANT4 modeling of the SD. The shower modeling functions are produced at each discrete energy and the zenith angle by generating approximately 1000 events at the arbitrary location of the SD array. Arbitrary numbers in energy and the zenith angle are obtained by the interpolation of discrete points. The model functions are generated for the primary proton using the QGSjet2 hadronization model.

The acceptance and the resolution of the reconstructed events are obtained by the same simulation.

V. Study of Systematics

The largest systematics in the energy determination comes from the ambiguity in the MC simulation used for the modeling. The differences of QGSjet2 and the DPMjet3[9], proton or Iron primaries are being studied using the above analysis method. There are different ways of shower reconstruction and the primary energy determination being adopted by past experiments. The AGASA used a semi-empirical lateral distribution function and the particle density at the core distance of 600m, S(600), as an energy estimator. The connection between the S(600) and the primary energy is obtained by the MC simulation and the attenuation of the S(600) with the zenith angle is obtained by applying the constant intensity cut (CIC) on the lower energy shower events. Such an analysis is being tried for the TA data with the energy estimator of S(800) and using a Corsika MC[10] with QGSjet2 and Sybil hadronization models.

We present the energy spectrum obtained by the above procedure and the estimates of the associated ambiguity in the coming conference in Lodz.

VI. Acknowledgement

The Telescope Array experiment is supported by the Ministry of Education, Culture, Sports, Science and Technology-Japan, Grant-in-Aid for Scientific Research on Priority Areas, The Origin of the Highest Energy Cosmic Rays, 2003, and for Scientific Research (B), 20340057, 2008. This experiment is also supported by the U.S. National Science Foundation (NSF) through awards PHY-0307098 and PHY-0601915 (University of Utah) and PHY-0305516 (Rutgers University) and by the Basic Research Program of the Korean Science and Engineering Foundation (KOSEF, Grant No. R01-2007-000-21088-0). The Dr. Ezekiel R. and Edna Wattis Dumke Foundation, The Willard L. Eccles Foundation and The George S. and Dolores Dore Eccles Foundation all helped with generous donations. The State of Utah supported the project through its Economic Development Board, and the University of Utah supported us through the Office of the Vice President for Research. The use of the experimental site became possible by the cooperation of the State of Utah School and Institutional Trust Lands Administration (SITLA), the federal Bureau of Land Management(BLM) and the United States Air Force. We also wish to thank the people and the officials of Millard County, Utah, for their steadfast and warm supports. We gratefully acknowledge the contributions from the technical staffs of our home institutions.

REFERENCES

[1] M. Takeda et.al., Phys. Rev. Lett. 81, 1163,(1998)
[2] T. Abu-Zayyad et.al, Phys. Rev. Lett. 92, 151101,(2004)
[3] K. Kasahara and F. Cohen, In Proc. 30th Int. Cosmic Ray Conf.,4, pages 581584, 2008.
[4] AMS Collaboration, Phys. Lett. B490, 27 (2000); Phys. Lett. B494, 193 (2000).
[5] S. Giani et al., Geant4: An Object-Oriented toolkit for Simulation in HEP, CERN/LHCC 98-44, 1998.
[6] T. Nonaka et.al., 2009, this conference
[7] E. Kido et.al., 2009, this conference
[8] S.Ostapchenko. . Nucl.Phys.Proc.Suppl., page 143, 2006.
[9] S. Roesler, R. Engel, J. Ranft, The Monte Carlo Event Generator DPMJET-III in Proceedings of the Monte Carlo 2000 Conference, Lisbon, October 2326 2000, A. Kling, F. Barao, M. Nakagawa, L. Tavora, P. Vaz eds., Springer-Verlag Berlin (2001) pp. 10331038.
[10] D. Heck et al. , Report FZKA 6019, Forschungszentrum Karlsruhe, 1998.